

Growth of $\text{In}_2\text{O}_3(100)$ on Y-stabilized $\text{ZrO}_2(100)$ by O-plasma assisted molecular beam epitaxy

A. Bourlange,¹ D. J. Payne,¹ R. G. Egdell,^{1,a)} J. S. Foord,¹ P. P. Edwards,¹ M. O. Jones,¹ A. Schertel,² P. J. Dobson,³ and J. L. Hutchison⁴

¹Chemistry Research Laboratory, Department of Chemistry, University of Oxford, Mansfield Road, Oxford OX1 3TA, United Kingdom

²Carl Zeiss SMT AG, Carl-Zeiss-Strasse 56, 73447 Oberkochen, Germany

³Oxford University Begbroke Science Park, Sandy Lane, Yarnton, Kidlington, Oxon OX5 1PF, United Kingdom

⁴Department of Materials, University of Oxford, Parks Road, Oxford OX1 3PH, United Kingdom

(Received 10 January 2008; accepted 31 January 2008; published online 7 March 2008)

Thin films of In_2O_3 have been grown on Y-stabilized $\text{ZrO}_2(100)$ by oxygen plasma assisted molecular beam epitaxy with a substrate temperature of 650 °C. Ordered epitaxial growth was confirmed by high resolution transmission electron microscopy. The position of the valence band onset in the x-ray photoemission spectra of the epitaxial films is found to be inconsistent with the widely quoted value of 3.75 eV for the fundamental bandgap of In_2O_3 and suggests a revised value of 2.67 eV. © 2008 American Institute of Physics. [DOI: 10.1063/1.2889500]

Indium oxide (In_2O_3) is one of the most important of all functional oxides. It is amenable to degenerate *n*-type doping to give a material which combines optical transparency in the visible region with a high electrical conductivity. Despite the ubiquitous application of Sn-doped In_2O_3 (the so-called indium tin oxide or ITO) as a transparent conducting contact in liquid crystal displays, solar cells, and electroluminescent display devices,^{1–4} relatively little effort has been directed toward the growth of high quality single crystal thin films of this material. To date, most work has concentrated on deposition of In_2O_3 on alumina⁵ and yttria-stabilized zirconia single crystal substrates by carefully controlled pulsed laser deposition^{6–8} (i.e., “laser” molecular beam epitaxy), although there are some reports of growth by more conventional molecular beam epitaxy (MBE) using oxygen atom plasma sources.^{9–11} Thus, many aspects of the fundamental physics of this important material remain controversial. For example, although early experimental work suggested that In_2O_3 has an indirect bandgap of about 2.62 eV,¹² the fundamental bandgap is widely quoted to be 3.75 eV or thereabouts, corresponding to the onset of strong optical absorption.^{13–15} Moreover, the most recent *ab initio* bandstructure calculations^{16,17} find no evidence of the upward dispersion of the valence bands required by the indirect gap hypothesis. In the present communication, we report the growth of In_2O_3 on Y-doped $\text{ZrO}_2(100)$ by radiofrequency (rf) oxygen plasma assisted molecular beam epitaxy. The face-centered cubic fluorite structure of Y-stabilized ZrO_2 belongs to the space group *Fm3m* with lattice parameter $a=5.1423$ Å at the 17% Y doping level of the substrates used in the current work. In_2O_3 has the bixbyite structure, being body-centered cubic with space group *I213*,¹⁸ and $a=10.1170$ Å. Thus, there is a small mismatch on the order of only 1.6% between $2a$ for Y-doped ZrO_2 (10.2846 Å) and a for In_2O_3 . Moreover, the two structures involve basically similar cation arrays but with $\frac{1}{4}$ of the anion sites of the fluorite structure vacant in In_2O_3 so that the cations are six coordinate rather than eight coordinate as in

fluorite. Thus, Y-doped ZrO_2 appears to be an ideal substrate for growth of well-ordered thin films of In_2O_3 . In the present work, epitaxial growth is confirmed by high resolution transmission electron microscopy (HRTEM) and selected area transmission electron diffraction. The valence band edge in x-ray photoemission spectroscopy of the epitaxial films is found to be 2.90 ± 0.05 eV below the Fermi level, which, in turn, lies at about 0.33 eV above the bottom of the conduction band due to defect induced *n*-type doping. These observations demonstrate that the fundamental bandgap is very much lower than the widely quoted value of 3.75 eV.

Indium oxide layers were grown on Y-stabilized $\text{ZrO}_2(100)$ substrates in an UHV oxide MBE system (SVT, Eden Prairie, MN) system with a base pressure of 5×10^{-10} mbar. This incorporated a conventional indium Knudsen cell and a radio frequency plasma oxygen atom source operated at 200 mW rf power with an oxygen background pressure of 5×10^{-5} mbar. The nominal deposition rate was set at 0.01 nm s^{-1} using a quartz crystal monitor offset from the sample position—the true growth rate on the sample was found to be about four times greater than this value. Substrates were heated radiatively using a graphite filament. They were cleaned by exposure to the oxygen atom beam with a measured substrate temperature of 900 °C. Films were then grown to a thickness of 120 nm at a substrate temperature of 650 °C. Complete coverage of the substrate was confirmed *in situ* using *N(E)* Auger spectroscopy and *ex situ* by x-ray photoemission spectroscopy. Thin slices for analysis by high resolution transmission electron microscopy were prepared in a Zeiss NVision 40 focused ion beam instrument incorporating a Ga liquid metal ion source and *in situ* Scanning EM imaging using a thermal field emission source. The areas selected for ion beam cutting were protected by an amorphous carbon overlayer and further covered with a Pt strap which was eventually welded to a micromanipulator probe to allow removal of the cut section and transfer to a copper grid. Finally, the slice was ion beam polished to electron beam transparency.

HRTEM observations were carried out using a JEOL 4000EX microscope operating at 400 kV. High resolution

^{a)}Electronic mail: russell.egdell@chem.ox.ac.uk.

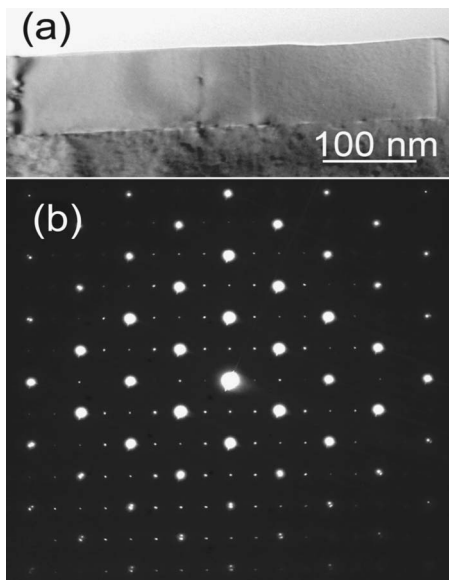


FIG. 1. (a) Low resolution cross sectional TEM image of In_2O_3 thin film on $\text{Y-ZrO}_2(100)$ substrate. In_2O_3 film is 125 nm thick. (b) Selected area electron diffraction pattern across the $\text{Y-ZrO}/\text{In}_2\text{O}_3$ interface. This indicates epitaxial matching of epilayer with the substrate.

x-ray photoemission spectra (XPS) were recorded in a Scienta ESCA 300 spectrometer which incorporated a rotating anode $\text{Al K}\alpha$ ($h\nu=1486.6$ eV) x-ray source. The x-ray source was run with 200 mA emission current and 14 kV anode bias, while the analyzer operated at 150 eV pass energy with 0.8 mm slits. Gaussian convolution of the analyzer resolution with a linewidth of 260 meV for the monochromated x-ray source gives an effective instrument resolution of 350 meV.

A low resolution cross sectional image of an In_2O_3 layer on the zirconia substrate is shown in Fig. 1(a). This reveals a dense crystalline film but with obvious macroscopic imperfections (e.g., at the left hand side of the image) suggesting incipient breakup of the film into micron sized islands. Nonetheless, selected area electron diffraction [Fig. 1(b)] indicated excellent crystalline order within the films, with well-defined spots between the main substrate reflections (face-centered cubic, in [011] projection) indicating a body-centered cubic cell, also in [011] orientation, with lattice parameter of approximately twice that of the Y-zirconia substrate. This is consistent with the bixbyite structure of In_2O_3 . Moreover, the near coincidence of substrate and epilayer spots demonstrates excellent epitaxial match between the In_2O_3 and the substrate.

High resolution cross sectional images are shown in Fig. 2. Figure 2(a) shows the interface region and reveals an abrupt, although not exactly flat, interface between the Y-stabilized ZrO_2 and the In_2O_3 . This observation is confirmed by both electron-energy-loss spectroscopy and energy dispersive x-ray microanalysis across the interface. Crystalline order is preserved up to the top surface, as shown in Fig. 2(b).

A valence band x-ray photoemission spectrum of an epitaxial In_2O_3 film is shown in Fig. 3 with alignment relative to a weak feature at the Fermi energy arising from population of the conduction band by adventitious donor defects, most probably oxygen vacancies. It is difficult from the experimental data to measure the width of the occupied part of the conduction band directly. However, from the integrated in-

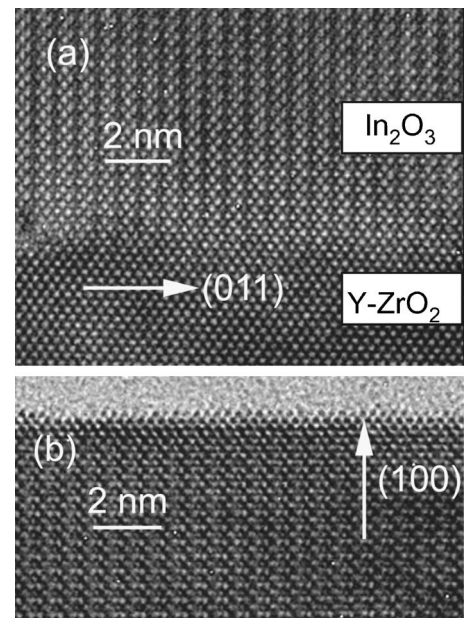


FIG. 2. (a) Cross sectional HRTEM image showing the $\text{Y-ZrO}_2(100)/\text{In}_2\text{O}_3$ interface. (b) HRTEM image showing that excellent crystalline order is preserved up to the top (100) surface of the In_2O_3 epilayer. The surface is almost atomically flat. The light contrast above the epilayer surface arises from the protective layer of amorphous carbon.

tensity of the conduction band feature relative to that of the valence band and from measurements of plasmon energies on $\text{In } 3d$ core lines,^{19,20} we can estimate that the carrier concentration n probed in the XPS experiment is of the order of $1.8 \times 10^{20} \text{ cm}^{-3}$. Assuming an effective mass m^* of $0.35m_0$ for the conduction band states, the width of the occupied part of the conduction band is then calculated to be 0.33 eV using the free electron model. This allows us to derive a value of $(2.90-0.33+R)$ eV for the fundamental bandgap of crystalline In_2O_3 , where R is the bandgap renormalization resulting from electron-electron and electron-impurity interactions. The earlier work of Hamberg *et al.*¹³ suggests a value for R

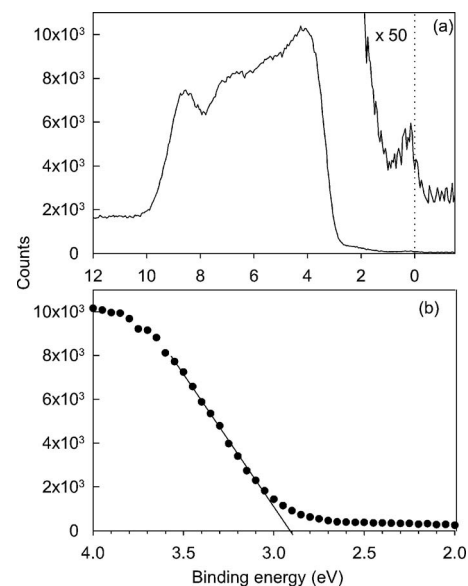


FIG. 3. (a) Valence band $\text{Al K}\alpha$ x-ray photoemission spectrum of epitaxial $\text{In}_2\text{O}_3(100)$ thin film. The spectrum has been aligned with reference to the weak feature arising from occupation of conduction band states. (b) Expansion of the valence band edge. Linear extrapolation, as shown, gives a valence band onset 2.90 ± 0.05 eV below the Fermi level.

of about 0.23 eV at our doping level, although very recent *ab initio* calculations give a lower value of at most 0.10 eV.²¹ Using the latter value, we obtain an estimate of 2.67 eV for the bandgap. This is very close to the value of 2.62 eV (Ref. 12) reported for the onset of weak optical absorption in bulk single crystal In₂O₃ but is very much less than the widely quoted value of 3.75 eV (Refs. 13–15) for the fundamental bandgap of In₂O₃. In the original work, the onset at 2.62 eV was associated with indirect optical transitions.¹² However, as discussed above, bandstructure calculations are inconsistent with the indirect gap hypothesis.^{16,17} Very recent theoretical and experimental work suggests that the shift between weak and strong absorption onsets is a consequence of the fact that transitions from the first six valence bands of In₂O₃ to the bottom of the conduction band are either dipole forbidden or contribute minimal dipole intensity to the absorption spectrum.²⁰ Thus, there is a difference of almost 1 eV between the fundamental bandgap and the onset of strong dipole allowed absorption. The present work adds weight to the conclusion that the valence band onset in XPS of In₂O₃ is, indeed, found to be very much less than 3.75 eV below the bottom of the conduction band. However, the previous work is based on data for magnetron sputtered thin films.²⁰ It is, therefore, reassuring to find that the same situation pertains for well-ordered (100) oriented thin films.

In summary, we have grown (100) oriented thin films of In₂O₃ on Y-stabilized zirconia thin films and confirmed that the valence band edge seen in x-ray photoemission lies at less than 3 eV below the Fermi energy. The results suggest a revised value for the bandgap of 2.67 eV. These conclusions are at variance with the hypothesis that the position of the valence band edge in photoemission experiments is determined by upward band bending associated with a metallic band of surface electronic states in the bulk bandgap.^{22,23}

This work was supported by EPSRC Grant No. GR/S94148 and the Scienta XPS facility by EPSRC Grant No. EP/E025722/1.

- ¹I. Hamberg and C. G. Granqvist, *J. Appl. Phys.* **60**, R123 (1986).
- ²C. G. Granqvist and A. Hultaker, *Thin Solid Films* **411**, 1 (2002).
- ³C. G. Granqvist, *Sol. Energy Mater. Sol. Cells* **91**, 1529 (2007).
- ⁴H. Hosono, *Thin Solid Films* **515**, 6000 (2007).
- ⁵M. Y. Chern, Y. C. Hunag, and X. L. Lu, *Thin Solid Films* **515**, 7866 (2007).
- ⁶H. Ohta, M. Orita, M. Hirano, H. Tanji, H. Kawazoe, and H. Hosono, *Appl. Phys. Lett.* **76**, 2740 (2000).
- ⁷H. Ohta, M. Orita, M. Hirano, and H. Hosono, *J. Appl. Phys.* **91**, 3547 (2002).
- ⁸T. Koida and M. Kondo, *J. Appl. Phys.* **99**, 123703 (2006).
- ⁹N. Taga, M. Maekwa, Y. Shigesato, I. Yasui, M. Kakei, and T. E. Haynes, *Jpn. J. Appl. Phys., Part 1* **37**, 6524 (1998).
- ¹⁰Z. X. Mei, Y. Wang, X. L. Du, Z. Q. Zeng, M. J. Ying, H. Zheng, J. F. Jia, Q. K. Xue, and Z. Zhang, *J. Cryst. Growth* **289**, 686 (2006).
- ¹¹U. Diebold and E. Morales (unpublished).
- ¹²R. L. Weiher and R. P. Ley, *J. Appl. Phys.* **37**, 299 (1966).
- ¹³I. Hamberg, C. G. Granqvist, K. F. Berggren, B. E. Sernelius, and L. Egström, *Phys. Rev. B* **30**, 3240 (1984).
- ¹⁴H. Köstlin, R. Jost, and W. Lems, *Phys. Status Solidi A* **29**, 87 (1975).
- ¹⁵S. Lany and A. Zunger, *Phys. Rev. Lett.* **98**, 045501 (2007).
- ¹⁶P. Erhart, A. Klein, R. G. Egdell, and K. Albe, *Phys. Rev. B* **75**, 153205 (2007).
- ¹⁷S. Z. Karazhanov, P. Ravindran, P. Vajeeston, A. Ulyashin, T. G. Finstad, and H. Fjellvag, *Phys. Rev. B* **76**, 075129 (2007), and references therein.
- ¹⁸M. Marezio, *Acta Crystallogr.* **20**, 723 (1966).
- ¹⁹V. Christou, M. Etchells, O. Renault, P. J. Dobson, O. V. Salata, G. Beamson, and R. G. Egdell, *J. Appl. Phys.* **88**, 5180 (2000).
- ²⁰A. Walsh, J. L. F. Da Silva, S. H. Wei, C. Körber, A. Klein, L. F. J. Piper, A. DeMasi, K. E. Smith, G. Panaccione, P. Torelli, D. J. Payne, A. Bourlange, and R. G. Egdell (unpublished).
- ²¹A. Walsh (unpublished).
- ²²A. Klein, *Appl. Phys. Lett.* **77**, 2009 (2000).
- ²³Y. Gassenbauer, R. Schafrank, A. Klein, S. Zafeirotas, M. Havecker, A. Knop-Gericke, and R. Schlogl, *Phys. Rev. B* **73**, 245312 (2006).